

Energy Dissipation Comparison of Normal Concrete Exterior Beam-Column Connection to that of ECC Connection Under Reversed Cyclic Loading

Muhammad Ishaq*, Zeeshan Ahmad

(Department of Civil Engineering, University of Engineering and Technology, Peshawar, Pakistan)

Email: mishaquetkp@gmail.com

Abstract:

This investigation aims to reveal the response of exterior beam-column joint regarding energy dissipation using engineered cementitious composites (ECC). Three full scaled type-2 (ACI-ASCE- 352) exterior beam-column connection were used to test under reverse cyclic loading (equivalent earthquake loading). Specimens were tested in control environment of load and displacement. Reversed cyclic load was applied on the tip of beam till failure stage. The damage pattern of crack was quite different in ECC used specimens regarding propagation and width compared to normal concrete (NC) specimen. Energy dissipation response was distinguishingly improved in ECC used specimens compared to NC used specimen.

Keywords —Exterior beam-column joint, reversed cyclic loading, engineered cementitious composite (ecc), energy dissipation

I. INTRODUCTION

During earthquake worldwide, the reinforced concrete beam-column joints failure was observed, where main cause was noted as inadequate confinement of joint [1]. Due to significant importance of beam-column joint in RC structures and its high ductility gain an attention of designers during worldwide occurred earthquakes [2]. To prevent any sudden failure of structures, beam-column joint would need an appropriate design to meet the strength and ductility requirements [3]. During earthquake loading, beam-column joint withstand different kind of stresses, dominantly shear stresses in multi kind of directions [4]. As per ACI-ASCE Committee-352 recommendations, the beam-column joint should be appropriately detailed with lateral steel hoops to prevent diagonal tension in beam-column joint zone [5]. The current amount of lateral steel reinforcement in joint zone caused steel congestion, which leads to difficulties in

construction practices of little compaction in joint zone and built a weak joint zone have less strength and sustainability during seismic activities [6-9]. Enormous researches have been done for improving RC beam-column joint using innovative design approaches and concepts for anchorage detailing and lateral steel hoops [1]. While very limited research has been done to used modern material like “Engineered Cementitious Composites (ECC)” and “High Performance Fiber Reinforced Cementitious Composites (HPFRCC)” to improve the lateral loading behavior in exterior beam-column connections [10-16].

This research work investigates the comparative response of engineered cementitious composites to normal concrete. In this study, used ECC as replacement material in joint /connection area instead of normal concrete to avoid the lateral steel congestion and make ease in construction practices. Particularly, this work extract the dissipated energy response when ECC is incorporated in exterior

beam-column connection/joint and subjected to cyclic loading. This work is the derivation of earlier limited work done on ECC usage to earthquake response.

RESEARCH OBJECTIVES

This study aims to reveal the structural usage of ECC instead of normal concrete in exterior beam-column joint subjected cyclic loading or equivalent earthquake loading. Furthermore, the energy dissipation and hysteretic damping in ECC incorporated specimens in comparison to normal concrete is the main objectives.

II. EXPERIMENTAL PROGRAM

a. Specimens Selection

Total three full scaled specimen T-type joints were fabricated and casted. One specimen was casted of normal concrete, while ECC were incorporated in two specimens (one joint zone and one in connection zone). Plywood kind of formwork were used for exterior beam-column connection to achieve straight edges and smooth surfaces. ECC incorporated zones and the dimensions of all specimens are shown in Figure. 01 (a & b) and Figure. 02 (a & b) respectively. The same details are elaborated in Figure. 02 (a & b). The reinforcement detailing is in compliance to ACI-318 detailing except lateral ties avoided in SJ-ECC core and SJ-ECC connection. Reinforcement details are shown in Figure-02 (a & b).

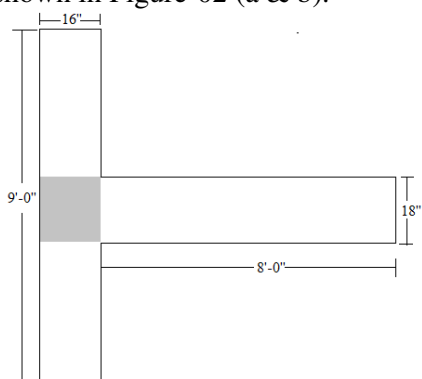


Figure 01 (a). SJ-ECC-I Joint (ECC incorporated area)

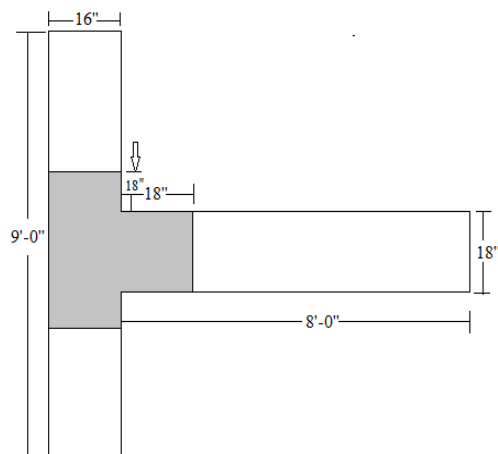


Figure 01 (b). SJ-ECC-II Connection (ECC incorporated area)

Figure 1 (a & b) Beam-column ECC zone Size and Dimensions

b. Mix Design

Mix was design for normal concrete while *Victor C. Li*ECC mix was modified for this part of work. Normal concrete and ECC table-01 proportions were used as design mix for compressive strength using Ordinary port land cement. The compressive strength obtained from mix design, used in this study were 3000 psi for NC and 6000 psi for ECC.

Table 1: Mix design Proportions for ECC and Normal Concrete

Mix	Cement	Fly Ash	Sand	Course aggregate	Water/Binder	Super Plasticizer	PVA Fiber
NC	1.0	--	2.5	3.2	0.55	--	--
ECC	1.0	1.2	0.8	--	0.37	0.046	0.028

Polyvinyl Alcohol Fiber (PVA) used in this research work manufacturer properties are shown in table 02 below.

Table 2: PVA manufacturer properties

Fiber Type	Length	Diameter	Aspect Ratio	Tensile Strength (MPa)	Elongation at Break(%)	Young's Modulus (GPa)
PVA REC15 x 8	8mm	40µm	200	1560	6.5	41

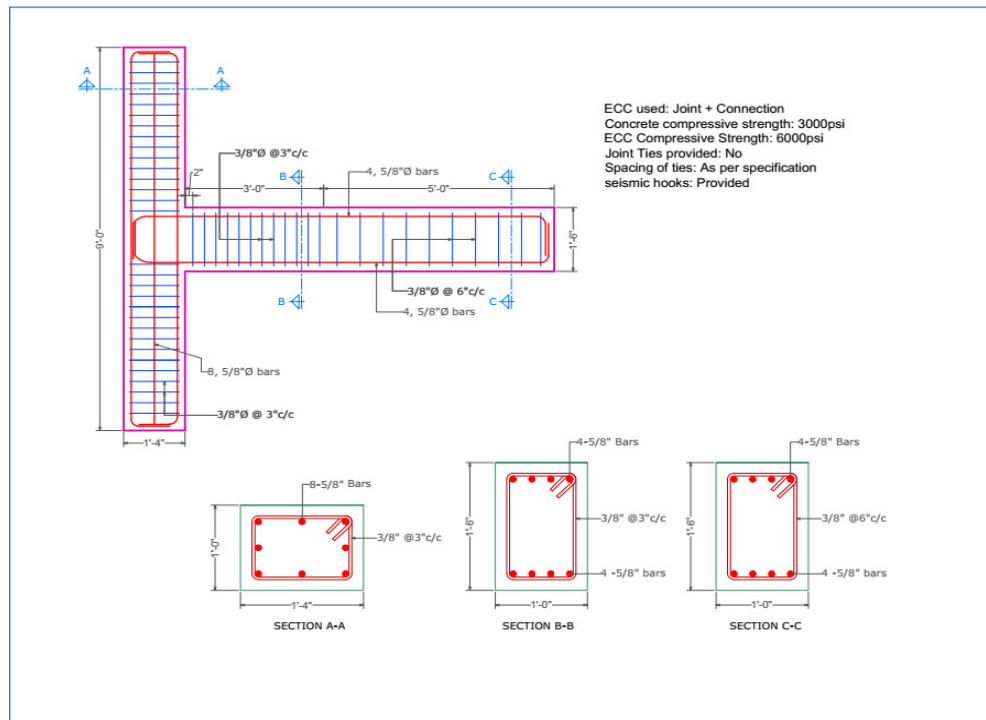


Fig. 02 (a) Specimens SJ-ECC-I & SJ-ECC-II joint and connection reinforcement details (no ties in joint core)

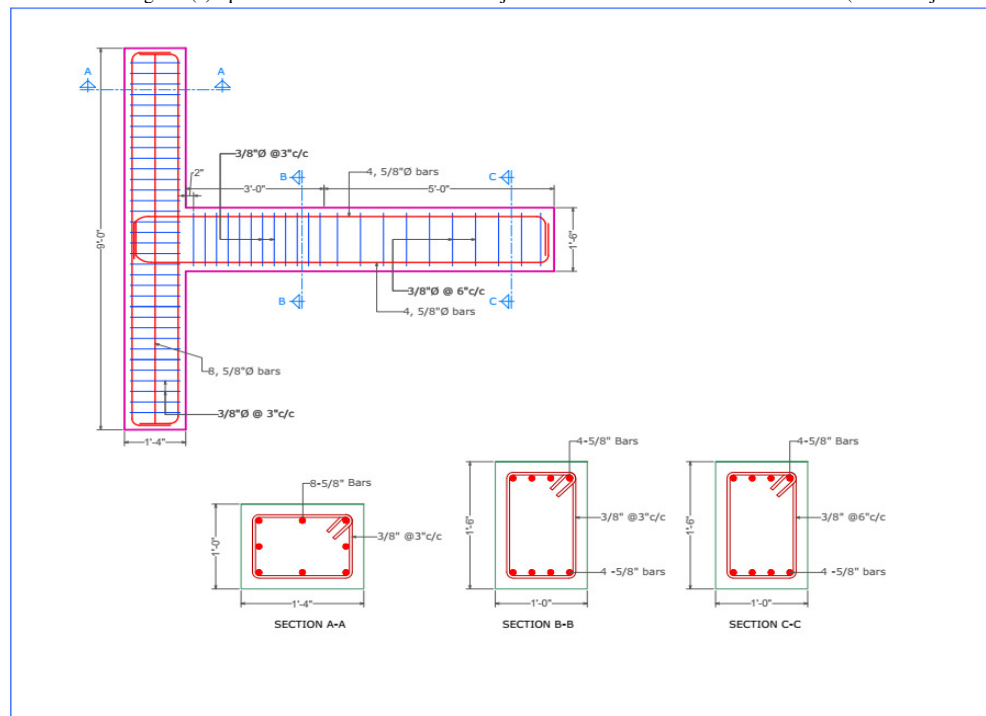


Fig. 02 (b) Specimens SJ-NC, reinforcement details
Figure 2 (a & b) Beam-column Size, Dimensions & reinforcement details

a. Materials Mixing and Pouring

The mixing steps for normal concrete was carried out by small mechanical mixture machine while ECC mixing was carried out manually. To gain proper workability of fresh concrete and ECC, the mixing was thoroughly done for two minutes of NC and for five of ECC. After homogeneous mix, the concrete was supplied to fabricated cages of steel and formwork shown in Figure. 02 (a & b). The ECC were poured only in joint and connection zones of specimens SJ-ECC core and SJ-ECC connection as shown in Figure. 03 (a) and (b) respectively. While the rest of specimens were poured with normal concrete. The concrete was poured in three layers in all specimens and thoroughly compacted through vibrator except the portion of joint and connection were separated by plates of steel. The specimens SJ-ECC joint zone and SJ-ECC connection zone were poured with ECC. Concrete and ECC were poured in the same time, while at the end ECC and concrete boundaries were carefully intermingled by vibrator. After 24 hours of casting, the specimens were covered by water retaining cloths. The water curing of specimens was carried out for 28 days to gain the design strength.



Fig 03. (a) ECC pouring in joint zone



Fig. 03 (b) ECC pouring in connection zone/plastic hinge zone

Figure 3 Portion of Exterior Beam-column Joint, a). ECC in joint, b). ECC joint and adjacent area

b. Testing protocol

Test specimens were strongly fit in the testing frame for testing. Figure. 04(a) and (b) presenting schematic and original lab setup respectively. The load cell used for cyclic load action at the tip of beam has capacity of 245 kN. The cyclic load action was applied at 7.5 ft. distance from the face of the support as shown in Fig. 04(a). A constant axial compressive load of magnitude 384 kN (15% of total axial compressive load) was applied to column by another load cell.

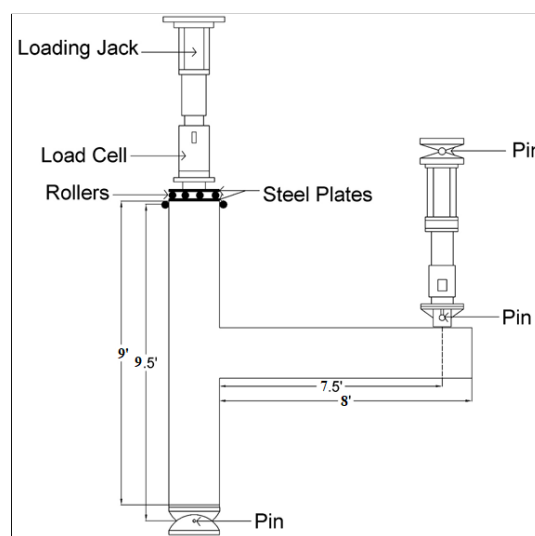


Fig. 04 (a)



Fig. 04 (b)

Figure 4 Testing Program, a) schematic setup, b) Lab setup

Displacement Transducers (DTs) and Linear variable differential transformer (LVDTs) were installed on specimens for recording parameters of interest. DTs and LVDTs were further attached to computer through data acquisition system.

The load application was arranged in two loading stages, load control stage and displacement control stage. Load control stage was further divide in four equal increments of $0.25F_y$, $0.50F_y$, $0.75F_y$ and F_y ($F_y = 3 \text{ Ton} = 29.43 \text{ kN}$). Similarly, displacement control stage was divided in drift ratio of 0.75%, 1.0%, 1.5%, 2.0%, 2.5%, 3.0%, 3.5%, 4.0%, 4.5%, 5.0%, 5.5%. Each load cycle was repeated three time.

III. RESULTS AND DISCUSSION

a. Failure Mode and Crack Pattern

i. Specimen SJ-ECC-I

The specimen faces were defined with West and East faces for recording of the crack pattern and failure mode. The reverse cyclic load was applied at in increment of $0.25F_y$ ($F_y = 29.43 \text{ KN}$) and increased to till $2.25 F_y$ and then to F_y . No crack was observed at first but minor cracks appeared at the $2.25F_y$ and F_y loading stages. After this control displacement of 0.75% of the 2438.4 mm was applied and first diagonal micro craze were observed. Similarly, control displacement was further increased to till 5.5% of the total drift of 2438.4mm and overall crack pattern was observed and noted as shown in Figure. 05 (a & b) of the west and east face of the specimen. After commencement of spalling, the test was terminated at 5.5% drift ratio.

ii. Specimen SJ-ECC-II

The specimen faces were defined with West and East faces for recording of the crack pattern and failure mode. The reverse cyclic load was applied at in increment of $0.25F_y$ ($F_y = 29.43 \text{ KN}$) and increased to F_y . No crack was observed at loading control stage. After this control displacement of

0.75% of the 2438.4 mm was applied and first diagonal micro craze were observed. Similarly, control displacement was further increased to till 5.5% of the total drift of 2438.4mm and overall crack pattern was observed and noted as shown in Figure. 06 (a & b) of the west and east face of the specimen. After 5.5% drift ratio, the test was terminated, with No spalling.



Fig. 05 (a)

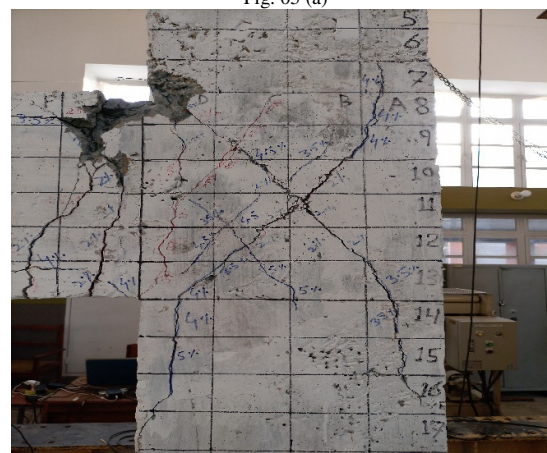


Fig. 05(b)

Figure 5. Crack pattern of specimen SJ-ECC-I, a). West face of the specimen, b) East face of the specimen

iii. Specimen SJ-NC

The specimen faces were defined with West and East faces for recording of the crack pattern and failure mode. The reverse cyclic load was applied at in increment of $0.25F_y$ ($F_y = 29.43 \text{ KN}$) and increased to till $2.25 F_y$ and then to F_y . No crack was observed at first but minor cracks appeared at

the 2.25Fy and Fy loading stages. After this control displacement of 0.75% of the 2438.4 mm was applied and first diagonal micro crack were observed. Similarly, control displacement was further increased to till 4.5% of the total drift of 2438.4mm and overall crack pattern was observed and noted as shown in Figure. 07 (a & b) of the west and east face of the specimen. After commencement of spalling, the test was terminated at 4.5% drift ratio.

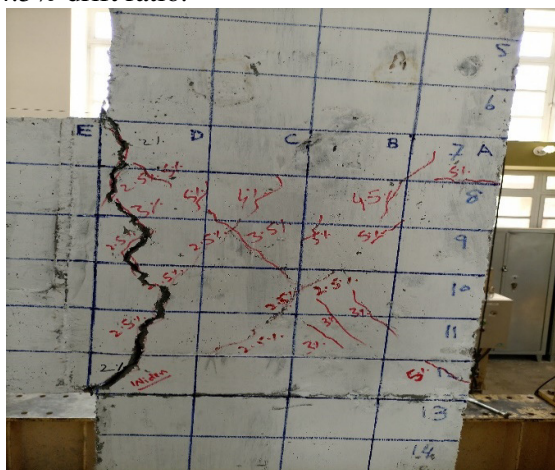


Fig. 06(a)

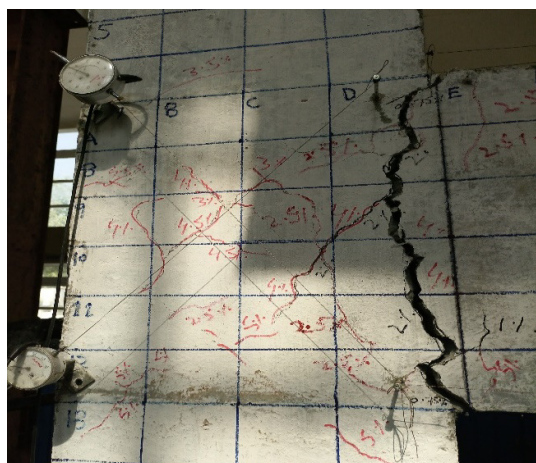


Fig. 06 (b)

Figure 6Crack pattern of specimen SJ-ECC-II, a). West face of the specimen, b) East face of the specimen



Fig. 07 (a)



Fig. 07 (b)

Figure 7Crack pattern of specimen SJ-NC, a). West face of the specimen, b) East face of the specimen

b. Accumulative Energy dissipation

Energy dissipation of all models was calculated from fore-deformation relationship curves by numerical integration. The relationship of accumulative dissipated energy per cycle and drift is shown in Figure 08. Drift is plotted on the x-axis while accumulative dissipated energy on the y-axis. The comparison of the three specimens also shown graphically in figure 08. The blue and green colour curves represent the ECC incorporated specimens while the orange colour represent the NC specimen. Accumulative energy dissipation comparison for model SJ-ECC-I, SJ-ECC-II and SJ-NC were 45461

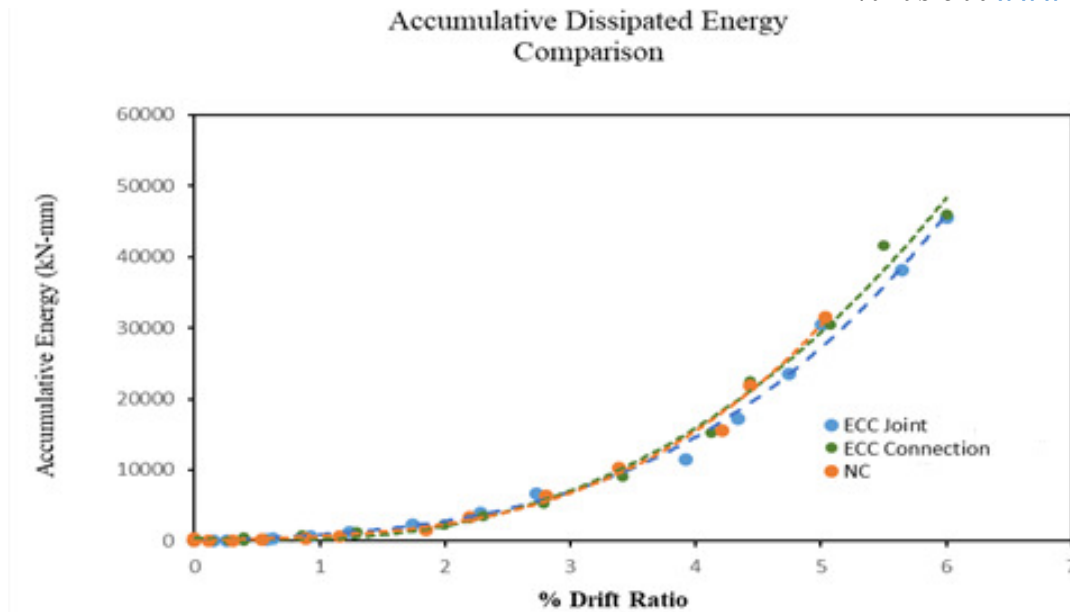


Figure 8 Accumulative Dissipated Energy Comparison of SJ-ECC-I, SJ-ECC-II, SJ-NC

KN-mm, 45940 KN-mm and 31505 KN-mm respectively.

tolerance at the ultimate stage of failure in contrast to NC.

IV. CONCLUSIONS

From the above experimental studies, the following conclusion were made:

1. Incorporation of ECC in the joint zone instead of NC, enhanced the performance of beam-column joint in term of ductility, shear resistance, damage tolerance and energy dissipation.
2. Overall cumulative dissipated energy of model SJ-ECC-I and SJ-ECC-II were increased by 44.5% and 45.82% respectively to SJ-NC. Hence, the result show that ECC has superior energy dissipation capacity relatively NC.
3. Model SJ-ECC-I and SJ-ECC-II test were almost terminated at 5.5% drift ratio, inspite the models joint fibers were in intact and were in good conditions but model SJ-NC was in the worse condition at 4.5% drift ratio. Hence, ECC was more damage

4. The global failure response of ECC joint and connection were ductile with strain hardening as compare to NC joint which was brittle with strain softening.

REFERENCES

- [1]. Pantelides CP, Hansen J, Nadauld J, Reaveley LD. Assessment of reinforced concrete building exterior joints with substandard details. PEER report 2002/ 18 Pacific Earthquake Engineering Research Center College of Engineering University of California, Berkeley; May 2002.
- [2]. N. Ganesan, P.V. Indira, R. Abraham, Steel fiber reinforced high performance concrete beam-column joints subjected to cyclic loading, J. Earthquake Technol. 44 (3-4) (2007) 445-456 (Technical Note)
- [3]. K.R. Bindhu, K.P. Jaya, Strength and behavior of exterior beam column joints with diagonal cross bracing bars, Asian J. Civ. Eng. (Build. Hous.) 11 (3) (2010) 397-410
- [4]. K.D.A. Ghani, N.H.A. Hamid, Comparing the seismic performance of beam-column joints with and without SFRC when subjected to cyclic loading, Adv. Mater. Res. 626 (2013) 85-89
- [5]. J.F. Bonacci, S.M. Alcocer, J.R. Cagley, J.M. LaFave, P. Paultre, M.E. Criswell, et al., Recommendations for Design of Beam-Column Connections in Monolithic Reinforced Concrete Structures, American Concrete Institute, 2002 (ACI 352R-02)
- [6]. C.H. Henager, Steel fibrous, ductile concrete joints for seismic-resistant structures, in: Symposium on Reinforced Concrete Structures in Seismic Zones, San Francisco, 1977, pp. 371-386
- [7]. T. Jiuru, H. Chaobin, Y. Kaijian, Y. Youngcheng, Seismic behavior and shear strength of framed joint using steel-fiber reinforced concrete, J. Struct. Eng. ASCE 118 (2) (1992) 341-358.
- [8]. R.J. Craig, S. Mahadev, C.C. Patel, M. Viteri, C. Kertesz, Behavior of Joints Using Reinforced Fibrous Concrete, vol. 81, ACI Special Publication, 1984 (pp. 125- 168).

- [9] A. Filiatrault, K. Ladicani, B. Massicotte, Seismic performance of code-designed fiber-reinforced concrete joints, *ACI Struct. J.* 91 (5) (1994) 564–571.
- [10]. Filiatrault A, Pineau S, Houde J. Seismic behavior of steel-fiber reinforced concrete interior beam–column joints. *ACI Struct J* 1995;92:543–52.
- [11] Shannag MJ, Barakat S, Abdul-Kareem M. Cyclic behavior of HPFRC-repaired reinforced concrete Interior beam–column joint. *Mater Struct* 2002;35:348–56.
- [12] Parra-Montesinos GJ, Peterfreund SW, Chao SH. Highly damage-tolerant beam–column joints through use of high-performance fiber-reinforced cement composites. *ACI Struct J* 2005;102:487–95.
- [13] El-Amoury T, Ghobarah A. Seismic rehabilitation of beam–column joint using GFRP sheets. *Eng Struct* 2002;24:1397–407.
- [14] Li B, Lam SSE, Wu B, Wang YY. Experimental investigation on reinforced concrete interior beam–column joints rehabilitated by ferrocement jackets. *Eng Struct* 2013;56:897–909.
- [15] Abbas AA, Mohsin SMS, Cotsovos DM. Seismic response of steel fibre reinforced concrete beam–column joints. *Eng Struct* 2014;59:261–83.
- [16] Gefken PR, Ramey MR. Increased joint hoop spacing in Type II seismic joints using fiber reinforced concrete. *ACI Struct J* 1989;86(2):168–72.